New Journal of Physics
The open–access journal for physics

Coupled surface plasmons and optical guided wave exploration of near-surface director profile

Fuzi Yang[1,2], Lizhen Ruan[2], S A Jewell[2] and J R Sambles[2]

[1] Department of Chemistry, Tsinghua University, Beijing 100084, People's Republic of China

[2] Thin Film Photonics, School of Physics, University of Exeter, Stocker Road, Exeter EX4 4QL, UK

E-mail: s.a.jewell@exeter.ac.uk

New Journal of Physics **9** (2007) 49
Received 7 December 2006
Published 5 March 2007
Online at http://www.njp.org/
doi:10.1088/1367-2630/9/3/049

Abstract. For a liquid crystal (LC) cell with thin silver claddings it is possible, using a high index coupling prism, to excite both surface plasmon modes and ordinary optical guided modes. In a situation where the tilt of the director varies from homogeneous to homeotropic through the cell, then for *p*-polarized incident radiation the *p*-polarized surface plasmon mode and the ordinary guided waves may couple to each other. When the plane containing the director is normal to the incident plane, there is also polarization conversion leading to strong coupling between the *p*-polarized surface plasmon and *s*-like guided modes. From theoretical analyses together with numerical modelling it is shown how this coupling between the surface plasmon mode and guided waves gives a high sensitivity to the surface director tilt profile near the walls, higher than that of the surface plasmon mode alone. Experimental confirmation of this has been realized using a hybrid aligned nematic (HAN) LC cell with the director in a plane normal to the incident plane. The results fully confirm the model predictions showing that this coupling of surface plasmons to guided waves provides a powerful tool for near-surface director studies.

PII: S1367-2630(07)38932-5

Contents

1. Introduction

Knowledge of the molecular director profile (the average molecular orientation) very near to the boundaries of a liquid crystal (LC) cell and its dynamic behaviour under external influence, e.g., an applied voltage, is key information to both fundamental research and practical device design. Various methods for detailed characterization of the surface director distribution have been explored for some years. Such procedures then allow for example, studies of the interaction between surface alignment materials and LC molecules [1], characterization of surface anchoring strength [2], quantification of flexo-electric effects [3], exploration of surface phase transitions [4] etc.

Widely regarded as one of the most powerful procedures is that of surface plasmon (or surface plasmon-polariton (SPP)) excitation [5]–[7]. As is well known, the SPP mode is a surface wave propagating at the interface between a metal and a dielectric. Its optical energy is confined to the interface, exponentially decaying into both media [8, 9]. The in-plane momentum of the SPP mode is very sensitive to the layers near the interface and thereby the SPP mode is a very good probe of optical parameters near a metal interface. Chu and Chen [10] appear to have been the first to use SPP excitation to characterize a LC, using the SPP on a gold layer to probe the nematic–isotropic phase transition. Chao *et al* [11] investigated cholesteric nematic LCs using a SPP on silver and, using also silver, Sprokel *et al* [12] explored the voltage dependence of the director tilt at the interface on which a SPP was excited. These early studies were on the excitation of SPP modes only. Oddly the study by Sprokel *et al* makes no mention of optical guided modes, which should also be found in their geometry. Welford and Sambles [13] appear to be the first to study of LCs to show both optical guided mode and SPP excitation using a single thin layer of silver in the Kretschmann–Raether geometry. Welford *et al* [14] appear also to be the first to use a symmetrical cladding of two thin silver layers on either side of the LC to excite surface plasmons on both interfaces as well as sharp fully-guided waveguide modes. The combined use of both SPP and guided mode excitation provides information about both near-surface and in-the-bulk director profiles.

Elston *et al* [15]–[18] continued this type of study exploring surface stabilized ferroelectric LCs for which the optical mode spectrum was far richer involving the excitation of SPPs and guided modes of two types, one set associated with the low index of the LC, another set with the high index. These studies appear to be the first to show that the SPP may interact with optical guide modes through polarization conversion due to the director geometry. This present study

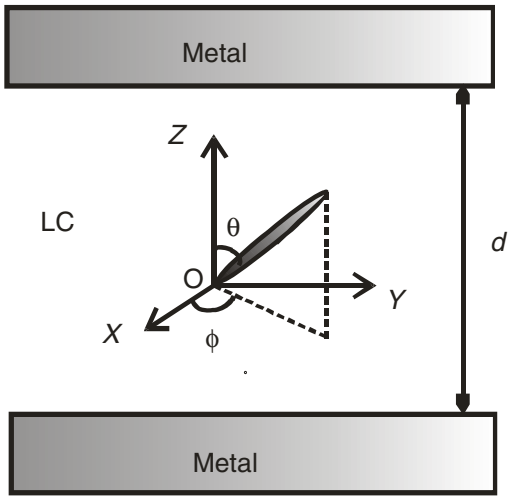

Figure 1. Schematic diagram of the geometry used in the metal-clad LC cell.

explores more completely this optical coupling between the two types of mode and shows that it may be used to reveal in great detail the near-surface director tilt profile.

In this study, a hybrid aligned nematic (HAN) LC cell clad symmetrically with thin films of silver is used to explore the coupling between the SPP mode and guided waves within the LC and thereby to study its usefulness as a near-surface director probe. The HAN structure has homogeneous alignment (director parallel to the substrate) at one surface and homeotropic alignment (perpendicular to the substrate) at the other, with the director tilting through approximately 90° across the cell.

Theory indicates that if the incoming radiation arrives at the homogeneously aligned side of the HAN cell and the LC director is tilted in a plane normal to the incident plane then, depending upon the director tilt profile the SPP mode, normally the highest in-plane-momentum *p*-polarized (transverse magnetic) mode for an isotropic dielectric, may overlie some of the *p*- and/or *s*-polarized (transverse electric) (created by polarization conversion) guided modes. For coupling between the SPP and *s*-polarized guided modes the conversion efficiency from the *p*-excited SPP to the *s*-type guided waves depends on several factors including the near surface tilt of the director, the ratio of the ordinary and extra-ordinary indices of the LC, the momentum and shape of the SPP mode etc. Over the SPP resonance the polarization conversion-excited *s*-like guided modes appear as sharp features that are very sensitive to the details of the near-surface director profile, more sensitive than the SPP itself.

2. Analysis

The model of a HAN LC cell symmetrically surrounded by thin silver layers is shown in figure 1. In the lab-frame *o-xyz* the molecular director tilt angle is θ and the twist angle is φ. For the HAN geometry the director is homogeneously aligned at the upper boundary and homeotropically aligned at the lower boundary of the cell. For a beam incident in the plane *zoy* with the director of the LC lying in the plane *zox* (out-of-plane $\varphi = 0°$) then for *p*-polarized incident radiation a SPP is excited at the top interface between the metal and the LC having in-plane momentum

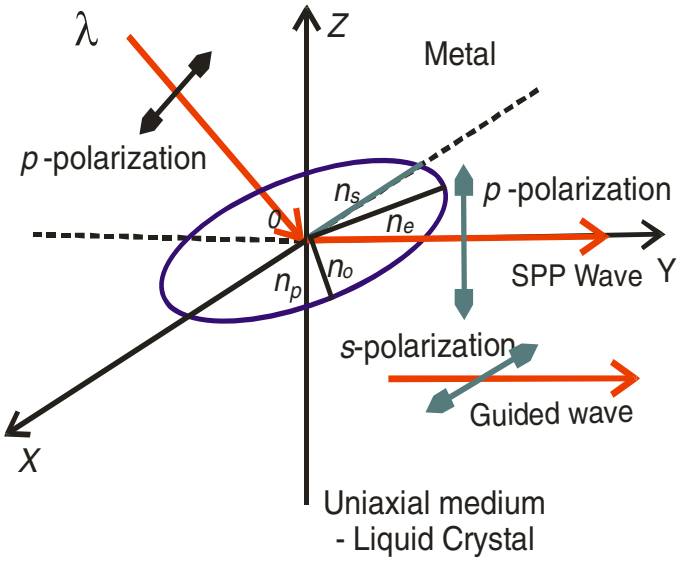

Figure 2. The surface plasmon mode and guided waves on the top-boundary area of a HAN cell relative to the orientation of the LC optic axes.

which is mainly dependent upon an effective index (see figure 2)

$$n_{\mathrm{p}} = \frac{n_{\mathrm{e}} n_{\mathrm{o}}}{\sqrt{n_{\mathrm{e}}^2 \sin^2\theta + n_{\mathrm{o}}^2 \cos^2\theta}} \tag{1}$$

Close to the upper boundary $\theta \approx 90^\circ$ and so $n_{\mathrm{p}} \approx n_{\mathrm{o}}$. If the director tilt of the LC material remains constant through the cell or it does not vary too quickly through the cell towards homeotropic alignment, as for a HAN cell under no or low external applied voltage, then the SPP is the highest in-plane momentum transverse magnetic (TM) mode and the other *p*-type guided modes are at lower angles. However, if there is a rapid variation of the director tilt in a very thin upper boundary area, even though it may only be a few degrees, strong *p* to *s* polarization conversion occurs and *s*-type guided modes may also be excited. The maximum in-plane momentum of this family of *s*-type guided modes is mainly dependent upon a different effective index (also see figure 2)

$$n_{\mathrm{s}} = \frac{n_{\mathrm{e}} n_{\mathrm{o}}}{\sqrt{n_{\mathrm{e}}^2 \cos^2\theta + n_{\mathrm{o}}^2 \sin^2\theta}} \tag{2}$$

As before, close to the upper boundary $\theta \approx 90^\circ$ and thus $n_{\mathrm{s}} \approx n_{\mathrm{e}}$. Therefore for a positive LC material having $n_{\mathrm{e}} > n_{\mathrm{o}}$, there is the possibility of *s*-polarized guided waves appearing in the angle range over which the SPP is excited. Because these *s*-polarized guided modes are converted from the *s*-polarized beam, then the *p*-polarized reflectivity will have sharp dips superimposed on the wider SPP mode minimum—a polarization coupling spectrum. For this *p* to *s* coupling spectrum between the *p*-polarized SPP mode and *s*-type guided waves the strength and position of these sharp *s*-type guided-mode features on the SPP response (these *s*-type modes are sharp because they are guided modes and also because there is very high reflectivity of the silver layers

to *s*-polarized light) depends strongly on the director tilt profile near to the upper metal surface and thereby they are particularly sensitive to the near-surface director tilt. Even with significant director tilt in the boundary area causing an increase of the SPP resonance angle and a decrease in the index sensed by the *s*-type modes this condition of the SPP mode overlapping with *s*-type guided modes may still remain valid. Indeed one may imagine that such overlap occurs provided the surface tilt is less than $\sim 45^\circ$. However, if the director tilt has already reached homeotropic alignment for much of the cell, as in a HAN cell under high applied voltage, then *p*-polarized guided modes with higher in-plane momentum may occur and these also may couple to the *p*-polarized SPP mode. This *p*–*p* coupling is not only dependent upon the director profile at the upper boundary but also upon the director behaviour in the bulk of the cell. In the next section, rigorous numerical modelling is used to confirm the above.

3. Modelling

For modelling the HAN LC layer is sandwiched between an input high index glass pyramid, on which are a thin silver film and a SiOx coating for aligning the LC, and a high index glass plate on the internal face of which is a second silver film and a thin lecithin layer. The incident radiation wavelength is 632.8 nm (He–Ne laser) and the optical parameters for the isotropic layers are, for the top glass pyramid $\varepsilon_{\mathrm{p}} = 3.2400$, for both thin silver films $\varepsilon_{\mathrm{Ag}} = -17.50 + \mathrm{i}0.65$, with thickness $d_{\mathrm{Ag}} = 45$ nm, for the SiOx coating $\varepsilon_{\mathrm{s}} = 2.550 + \mathrm{i}0.002$ with thickness $d_{\mathrm{s}} = 25$ nm and for the bottom glass plate $\varepsilon_{\mathrm{g}} = 3.2400$. The uniaxial LC has $\varepsilon_{xx} = \varepsilon_{yy} = 2.2306 + \mathrm{i}0.0002$ and $\varepsilon_{zz} = 3.0285 + \mathrm{i}0.0002$ with a thickness of $d_{\mathrm{LC}} = 12.00\,\mu$m having a tilt angle which varies from $\theta_1 = 90.0^\circ$ at the top to $\theta_2 = 0.0^\circ$ at the bottom with a constant twist angle φ. The very thin lecithin layer can be ignored as far as its optical effect is concerned.

With no voltage applied to the cell the tilt angles of the LC layer is modelled to vary linearly from the top ($\theta_1 = 90.0^\circ$) to the bottom ($\theta_2 = 0.0^\circ$). Now consider a thin layer of thickness $0.40\,\mu$m at the top boundary in which the tilt angle has two other different profiles, curves labelled 2 and 3, compared with the linear variation of curve 1, as shown in figure 3. Consider first, the out-of-plane geometry ($\varphi = 0.0^\circ$). The computed reflectivity curves for R_{pp} are shown in figure 4, the solid line is the response for profile 2 and the dashed line that for profile 3. It is very clear that the optical responses, caused by these two director profiles, are readily distinguished by the coupling spectrum. Profile 3, for which the director gradient is larger near the top boundary, leads to stronger *p*- to *s*-polarization conversion (arising due to the uniaxial nature of the material) than profile 2. To explore the physics the optical *E*-field distributions for the two cases at an incident angle β_1 (see figure 4) are calculated and shown in figure 5(a) and (b), respectively. It is very clear that because the penetration depth of the *p*-polarized SPP mode is about 0.25–$0.30\,\mu$m, then for case 3 there is a much stronger *p*-polarized field in the rapidly varying region of director tilt which converts to stronger *s*-polarized guided modes than in case 2 thus giving deeper features in the SPP mode profile.

If the sample is rotated around the *z*-axis by 90.0°, to the in-plane situation, then indistinguishable reflectivity signals R_{pp} are predicted for both profiles 2 and 3. Thus the conventional SPP resonance cannot be used to distinguish the two profiles of the director near the boundary area. Indeed inspection of figure 4 also reveals this, for it is really only the sharp polarization converted modes which are different in the out-of-plane case, the broad SPP resonance itself being unchanged.

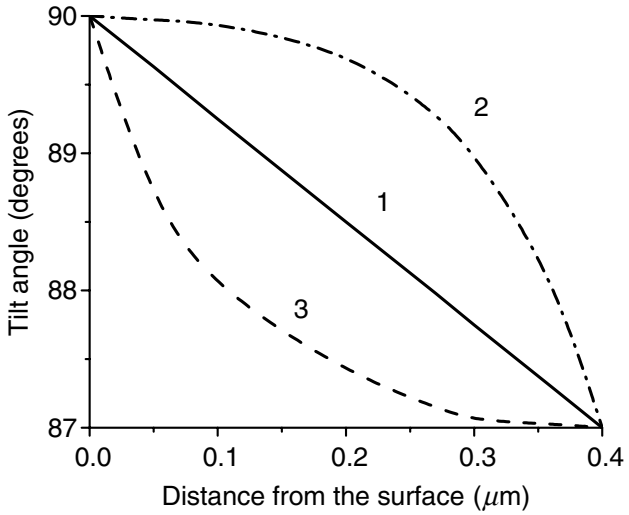

Figure 3. The three different situations of the tilt angle distributions near the top-boundary area of the HAN cell used for the computed reflectivity curves shown in figure 4.

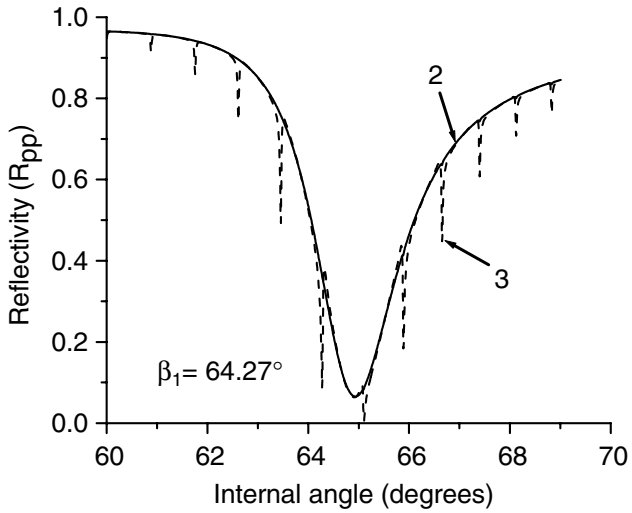

Figure 4. The modelling results of the reflectivity (R_{pp}) in the surface plasmon mode area for different tilt angle profiles.

Furthermore fully-leaky LC waveguide measurements using high index walls with no silver layers are also incapable of distinguishing these two profiles. The data are indistinguishable for the two situations. It would therefore appear that polarization coupling between the *p*-like SPP mode and *s*-like guided modes is an excellent waveguide method for exploring the director distribution near the boundary of a LC cell. In the next section, this result is shown experimentally.

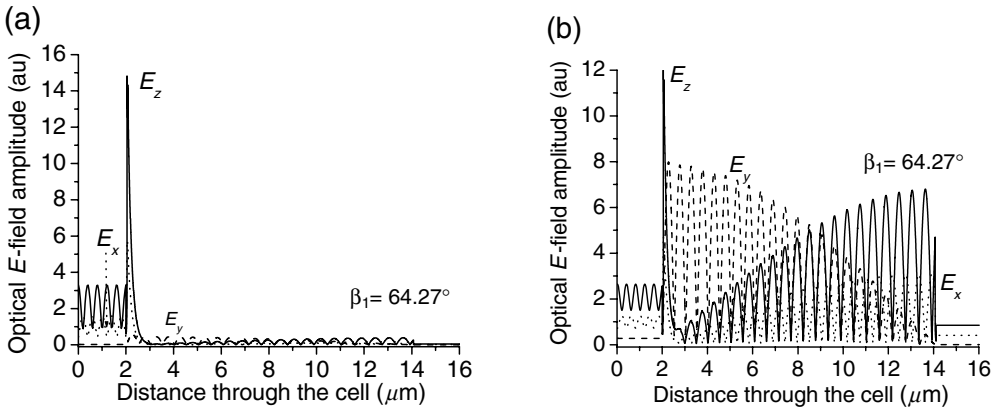

Figure 5. The optical E-field distribution through the cell at incident angle β_1 shown in figure 4. (a) For case 2 and (b) for case 3, respectively. In both cases the LC extends from 2.0 to 14.0 μm.

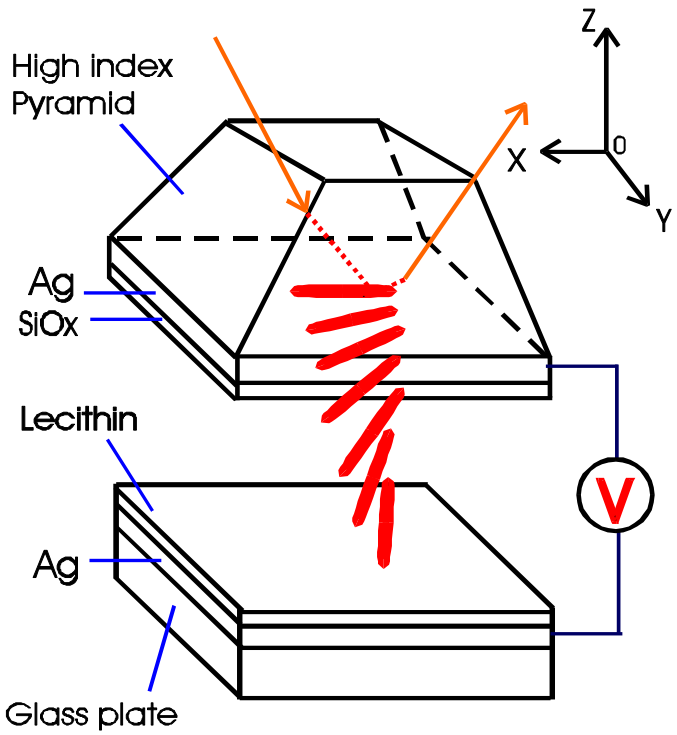

Figure 6. The experimental sample geometry.

4. Experiment

A symmetrical silver clad HAN LC cell has been built to test the above results. The sample geometry is shown in figure 6. A high index glass pyramid and a glass plate are used as the cell top and bottom walls with the pyramid also used as the optical coupling element. Inner surfaces of both the pyramid and the plate first have evaporated on to them thin silver layers (∼43 nm). This is followed by a 60° evaporated SiOx thin film on the silver film on the pyramid, giving

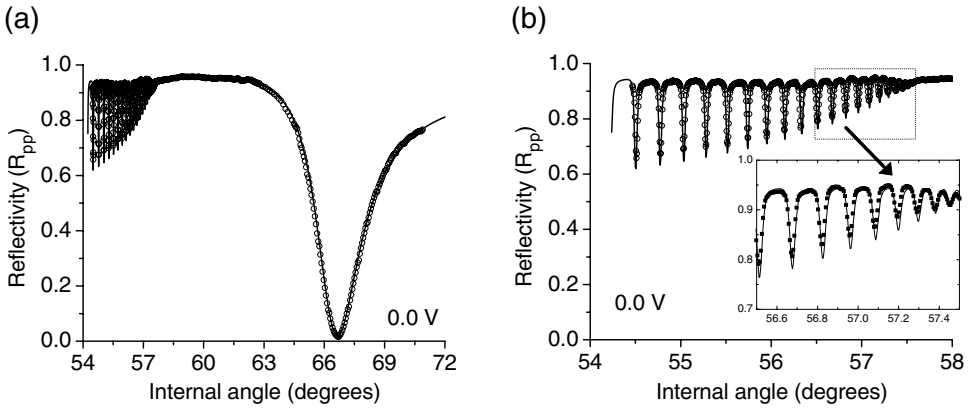

Figure 7. (a) The whole incident angle range of the reflectivity, R_{pp}, data (circles) and fitting result (solid line) for no voltage. (b) The guided mode range of the above situation shown on an expanded scale.

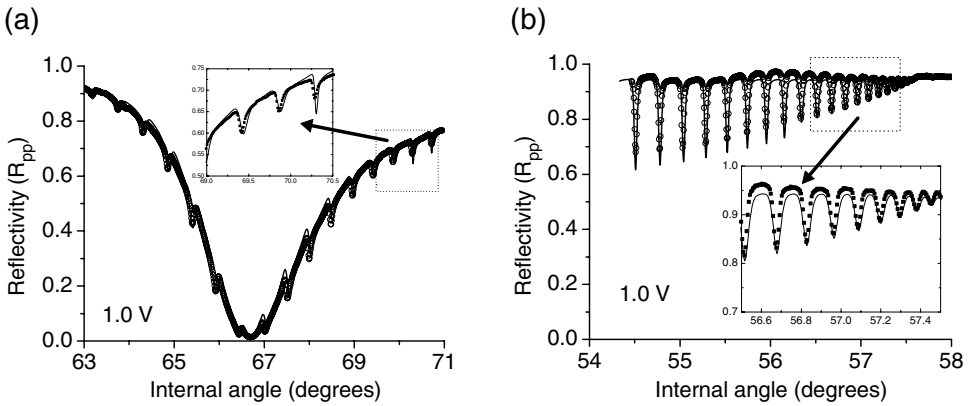

Figure 8. (a) The surface plasmon mode area reflectivity, R_{pp}, data (circles) and model fit (solid line) at 1.0 V. (b) The guided mode range reflectivity, R_{pp}, data (circles) and model fit (solid line) at 1.0 V.

homogeneous alignment, and a lecithin layer is deposited from ether solution on the silver film on the bottom plate to act as a homeotropic alignment layer. Two mylar strips with thickness about 15.0 μm are used as the cell gap spacers and the cell is capillary filled with the nematic LC of positive dielectric anisotropy (E7, Merck-BDH) at room temperature.

The experimental set-up is a typical θ–2θ rotatable system as described elsewhere [14, 15]. A 632.8 nm red radiation beam from a He–Ne laser first passes through a polarizer, creating a *p*-polarized incoming beam on one pyramid face. Then the incident angle-dependent reflectivity signals are recorded by a detector with a *p*-polarizer in front of it with different applied voltages across the cell from 0.0 to 3.5 V at 0.5 V intervals using a frequency of 10 kHz. Typical recorded R_{pp} signals are shown in figures 7–9 as circles for applied voltages of 0.0, 1.0 and 1.5 V, respectively.

The theoretical fitting results are also shown in figures 7–9 as solid lines. In figure 8(a) the whole angle range spectrum which includes the TM-like guided modes and the SPP mode is

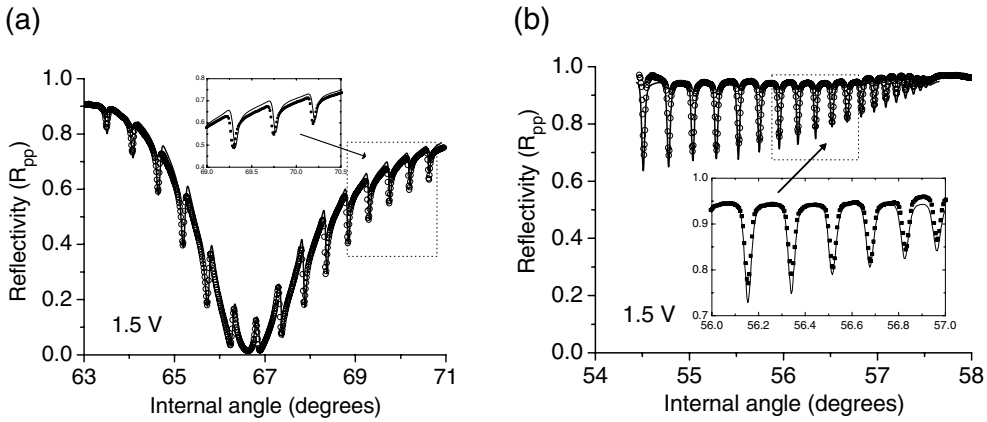

Figure 9. (a) The surface plasmon mode area reflectivity, R_{pp}, data (circles) and model fit (solid line) at 1.5 V. (b) The guided mode range reflectivity, R_{pp}, data (circles) and model fit (solid line) at 1.5 V.

shown while in figure 7(b) is the detail of the TM-like guided waves area. Fitting a predicted response, using a 4×4 scattering matrix model to this whole range with no voltage applied gives the basic parameters of the geometry. With a known glass permittivity of 3.2400, the parameters from the fitting are that for the silver films $\varepsilon_{Ag} = -17.85 + i0.995$, $d_{Ag} = 43.0$ nm, SiOx aligning layer $\varepsilon_s = 2.5500 + i0.002$, $d_s = 25.0$ nm, LC E7 $\varepsilon_{xx} = \varepsilon_{yy} = 2.3108 + i0.0002$, $\varepsilon_{zz} = 3.0165 + i0.0002$, $d_{LC} = 17.40\,\mu$m with twist angle $\varphi = 0.0^\circ$ (out-of-plane geometry) with a tilt angle which varies linearly from the top boundary ($\theta_1 = 90.0^\circ$) to the bottom boundary ($\theta_2 = 0.0^\circ$). Fits are also done for each set of data at applied voltages of 1.0 and 1.5 V. The elastic constants and anisotropic dielectric permittivity are chosen as $K_{11} = 14.20$ N, $K_{33} = 18.20$ N, $\varepsilon_\parallel = 19.50$ and $\varepsilon_\perp = 5.40$ for the LC E7 at room temperature and the tilt anchoring strength $W_{\theta 1} = 1.5 \times 10^{-4}\,\mathrm{J\,M^{-2}}$ on the upper aligning boundary and $W_{\theta 2} = 2.0 \times 10^{-3}\,\mathrm{J\,M^{-2}}$ on the bottom boundary. Figures 8 and 9 are typical fitted results shown as solid lines for applied voltages of 1.0 and 1.5 V respectively. Figure 10(a) shows the fitted tilt angle profiles through the cell under applied voltages of 0.0, 1.0 and 1.5 V modelled using continuum elasticity theory [19].

Figure 10(b) shows the detail of the tilt angle variation at the upper boundary area for the case 1, 2 and 3 with 0.0, 1.0 and 1.5 external volts. From figure 10(b) it is clear that the surface tilt angles deviate from horizontal ($\theta_1 = 90^\circ$) due to the balance between surface anchoring and elastic forces due to E-field coupling to the director. If the surface anchoring force at the upper surface is very strong, thereby keeping the surface tilt angle at 90.0°, then the tilt profile shown as the dotted line 4 in figure 10(b) with no change in the remainder of the cell may be imagined. In which case the coupling spectrum still distinguishes between that and curve 3, as shown by figure 10(c) in which the solid line predicted from curve 4 is compared with the experimental data (circles). However, the envelope of the SPP mode does not change at all for both cases 3 and 4 as shown in figures 9(a) and 10(c). This demonstrates the sensitivity of the coupling spectrum to the surface director profile and also obviously indicates that the surface tilt angle profile predicted by the continuum theory is reasonable.

Further results at higher voltage are also interesting. Figure 11(a) shows the experimentally recorded reflectivity, R_{pp} data in the SPP mode region, at 3.5 V. There is very strong coupling

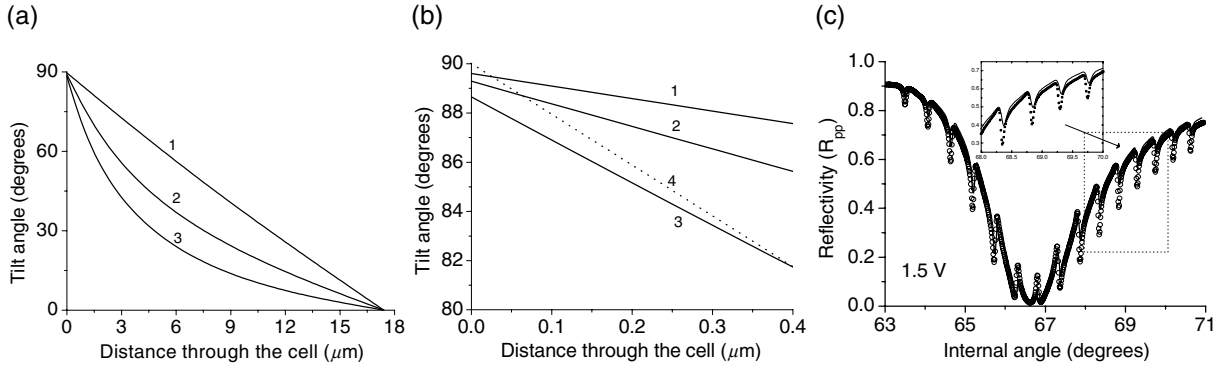

Figure 10. (a) The tilt angle distribution through the cell under voltages of 0.0, 1.0 and 1.5 V. (b) The detail of the tilt angle distribution near the upper boundary. The solid curves 1, 2 and 3 are for 0.0, 1.0 and 1.5 V, respectively. The dotted curve 4 is an imaginary profile with the surface tilt fixed at 90°. (c) The model coupling spectrum (solid line) for the tilt angle distribution as shown in (b) by the dotted line (case 4) compared with experimental data (circles).

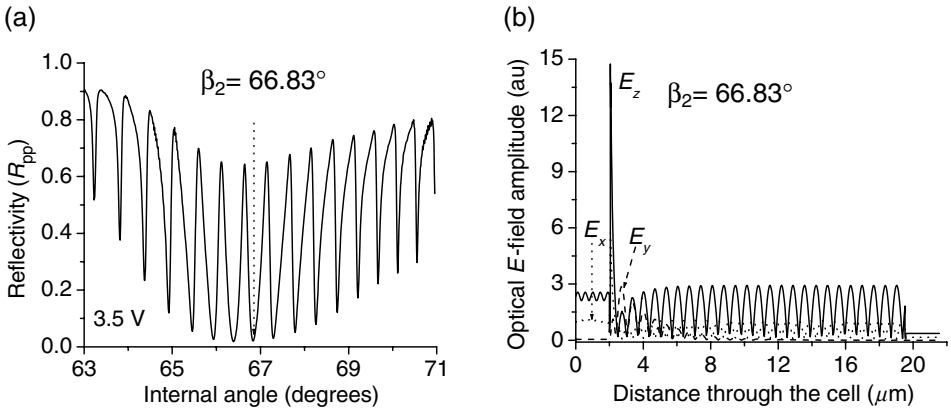

Figure 11. (a) The experimentally recorded reflectivity R_{pp} at 3.5 V. (b) The optical E-field distribution at a chosen incident angle β_2 (see (a)).

between the SPP mode and the p-like guided waves. This is confirmed from the optical E-field distribution calculated at one of mode angles ($\beta_2 = 66.83^\circ$ see figure 11(a)) as shown in figure 11(b). This indicates that at these voltages most of the optical E-field through the cell is p-type. However, because there is still some p- to s-conversion in the upper surface area and the behaviour of the guided wave is also dependent upon the E-field distribution through the whole cell, these p–p type coupling spectra are also quite sensitive to the director profile at the upper boundary area. We will discuss this matter in further papers.

5. Conclusions

Theoretical analyses and numerical modelling have shown that for a symmetrical metal-clad HAN LC cell and p-polarized incident radiation the polarization coupling spectrum between

s-type guided waves and the *p*-polarized surface plasmon mode is a very sensitive probe for exploring the director profile near to the boundary. By using this spectrum very small changes of the director profile near the boundary area can be distinguished, even though the surface plasmon mode itself is not sensitive to these changes (neither are the ordinary guided waves).

Experimental results from a symmetrical silver-clad HAN LC cell containing E7 have confirmed the analytic and model predictions and show how the top-surface director profile varies at lower applied voltages. This use of the polarization conversion spectrum through the excitation of an SPP together with other guided modes can be easily extended to studying the dynamic behaviour [20] of the surface director and thus it will be a very powerful tool for surface LC physics research.

Acknowledgments

We are pleased to acknowledge the support of The Royal Society for this British–Chinese cooperative study.

References

[1] Jewell S A and Sambles J R 2002 *J. Appl. Phys.* **92** 19
[2] Yang F Z, Ruan L Z and Sambles J R 2000 *J. Appl. Phys.* **88** 6175
[3] Jewell S A and Sambles J R 2003 *Mol. Cryst. Liq. Cryst.* **401** 181
[4] Ruan L Z, Osipov M A and Sambles J R 2001 *Phys. Rev. Lett.* **86** 4548
[5] Jorgenson R C and Yee S S 1993 *Sensors Actuators* B **12** 213
[6] Cheng S F and Chau L K 2003 *Anal. Chem.* **75** 16
[7] Sharma A K and Gupta B D 2006 *Nanotechnology* **17** 124
[8] Otto A 1968 *Z. Phys.* **216** 398
[9] Kretschmann E 1971 *Z. Phys.* **241** 313
[10] Chu K C and Chen C K 1980 *Mol. Cryst. Liq. Cryst.* **59** 97
[11] Chao N-M, Chu K C and Shen Y R 1981 *Mol. Cryst. Liq. Cryst.* **67** 261
[12] Sprokel G J, Santo R and Swalen J D 1981 *Mol. Cryst. Liq. Cryst.* **68** 29
[13] Welford K R and Sambles J R 1987 *Appl. Phys. Lett.* **50** 871
[14] Welford K R, Sambles J R and Clark M G 1987 *Liq. Cryst.* **2** 91
[15] Elston S J, Sambles J R and Clark M G 1989 *J. Mod. Opt.* **36** 1019
[16] Elston S J and Sambles J R 1990 *J. Appl. Phys. Japan* **29** L641
[17] Elston S J and Sambles J R 1991 *Ferroelectrics* **113** 325
[18] Elston S J and Sambles J R 1991 *Mol. Cryst. Liq. Cryst.* **200** 167
[19] Leslie F M 1970 *Mol. Cryst. Liq. Cryst.* **12** 57
[20] Yang F, Dong Y, Ruan L Z and Sambles J R 2004 *J. Appl. Phys.* **95** 310